Effect of Composition on the Corrosion Behavior of Stainless Steels Brazed with Silver-Base Filler Metals

An electrochemical galvanic action between coexisting phases is responsible for the corrosion of filler metal and interface

BY T. TAKEMOTO AND I. OKAMOTO

ABSTRACT. The effect of composition of silver-base filler metals and austenitic stainless steels on the corrosion of stainless steel joints brazed with silver-base filler metals was investigated in aqueous sodium chloride solution. The depth of corrosion in the filler metal increased with the increase of zinc content in filler metal and (Ni + Cr) content of base metal. The interfacial corrosion was promoted by the increase of silver content in the filler metal.

The phenomena are explained by the galvanic cells such as the stainless steel bulk surface/α-Cu phase in filler metals, and the α_1-Ag phase/active stainless steel at the braze interface. The brazing flux leaves the active layer at the braze interface by the removal of protective passive films; this is believed to be one of the causes of interfacial corrosion.

A nickel-depleted ferrite phase is observed at the interface brazed with nickel-free filler metals; however, the formation of a nickel-depleted zone is prevented by the use of filler metals with 2% Ni. Addition of nickel to filler metals is found to prevent the formation of the less corrosion resistant nickel-depleted zone.

Introduction

Stainless steel joints brazed with silver-base filler metals have been widely employed for piping, industrial heat exchangers and other conventional joints. The joints are expected to be corrosion resistant in the atmosphere containing moisture, aggressive gases and chloride ions. However, these joints have been known to fail by interfacial corrosion. Sistare *et al.* tested the corrosion resistance of Type 430 stainless steel joints (brazed with silver-base filler metals) in running tap water and paid attention to the corrosion at the braze interface (Ref. 1). They considered the interfacial corrosion was similar to the crevice corrosion which was accelerated by the formation of an oxygen concentration cell. They used 40 kinds of silver-base filler metals and recommended several relatively corrosion resistant filler metals containing nickel.

Kawakatsu (Ref. 2) evaluated the corrosion resistance of Type 430 and 304 stainless steel joints brazed with silver-base filler metals. He did this by measuring the decrement of tensile strength after immersion in various acids and alkaline aqueous solutions. This work pointed out that a nickel-rich layer was formed along the interface in nickel bearing BAg filler metal joints; it stated that the layer was responsible for the improvement of corrosion resistance. Other work also referred to the advantageous effect of nickel additions to filler metals on joint life (Ref. 3) and dezincification in sea water (Ref. 4). The use of zinc-free, nickel-bearing filler metal is also found to be beneficial (Refs. 5,6,7).

The selection of appropriate combinations of silver-base filler metal and stainless steel appears to be important to improve the corrosion resistance of stainless steel brazed with silver-base filler metals. However, even the fundamental aspects concerning the effect of composition of Ag-Cu-Zn ternary filler metals and stainless steel composition and also the improvement mechanism by nickel addition on the corrosion resistance of stainless steels brazed with silver-base filler metals has not yet been clarified sufficiently.

The joint is usually made by the aid of flux to remove the passive oxide films and thereby permit intimate contact between filler and base metal. Hence, the stainless steel is brazed to filler metal after removal of the protective passive film without repassivation; this leaves the thin active layer in stainless steel base metal at the interface. In addition to this, at the braze interface, various phases with different electrochemical properties such as α_1-Ag, α-Cu, and austenite (passive surface and active interface) coexist; this suggests galvanic corrosion cells may function among them.

This paper describes the effect of Ag-Cu-Zn ternary silver filler metal composition and stainless steel composition on the corrosion behavior of brazed joints. It does so by considering the metallurgical factors and electrochemical galvanic effects. The improved mechanism resulting from nickel addition to silver filler metals was also investigated.

Table 1—Chemical Composition of Filler Metals, Wt-%

Filler metals	Ag	Cu	Ni	Zn	Brazing temperature °C	(°F)
BAg-6	50.50	34.90	–	Balance	800	(1472)
BAg-5	45.11	30.53	–	Balance	800	(1472)
CF-12[a]	40.47	30.38	–	Balance	800	(1472)
BAg-4	39.89	30.86	2.05	Balance	830	(1526)

(a) Laboratory number.

Paper presented at the 15th International AWS-WRC Brazing and Soldering Conference held in Dallas, Texas, during April 10-12, 1984.

T. TAKEMOTO is Research Instructor and I. OKAMOTO is Professor, Welding Research Institute, Osaka University, Osaka, Japan.

Table 2—Chemical Composition of Stainless Steel Base Metals, Wt-%

Type stainless steel base metal	Element[a]								
	Ni	Cr	C	Si	Mn	P	Ti	Mo	Fe
304	8.71	18.04	0.06	0.61	1.04	0.029			Balance
304L	10.29	18.17	0.014	0.65	1.60	0.030			Balance
321	9.10	17.15	0.06	0.66	0.96	0.031	0.31		Balance
316	11.80	17.07	0.05	0.80	1.02	0.025		2.65	Balance
309	14.29	22.59	0.06	0.70	1.56	0.040			Balance
310S	19.80	24.64	0.06	0.73	1.68	0.024			Balance

(a) S—0.001 to 0.009.

Experimental Procedures

The chemical compositions of filler metals and stainless steels are presented in Tables 1 and 2, respectively. The machined dimensions (in mm) of the stainless steel base metals were: thickness—8, width—12, and length—60 (0.315 × 0.47 × 2.36 in.) with a center groove of 2.5 mm (0.1 in.) radius.

The filler metals and commercial brazing flux were put in the groove. They were heated to the brazing temperature in an air atmosphere furnace and held for 1 min and then air cooled. Prior to the brazing, the materials were rinsed in an acetone-ultrasonic bath. After brazing, the specimens were rinsed in warm water to remove the flux residues.

The brazed specimens were then cut to 15 mm (0.59 in.) lengths and polished with no. 600 emery paper and subjected to immersion type corrosion test—Fig. 1. The specimens were designed to eliminate voids at the brazed interfaces. Also, the area where filler metal thinly spread was eliminated by polishing. The specimens made it possible to measure the interfacial corrosion length and corrosion depth of filler metal, respectively, and were useful to discussion of the corrosion mechanism.

Corrosion tests were carried out using 0.4 mol/liter NaCl + 0.005 mol/liter $CuCl_2 \cdot 2H_2O$ aqueous solution; the temperature was maintained at 25°C (77°F) by a controlled water bath. After immersion for certain days in test solution, specimen cross sections were examined by an optical microscope and a profile projector with digital read-out facility.

Metallurgical studies using an x-ray diffractometer and scanning electron microscope with an energy dispersive x-ray analyzer, and electrochemical studies were also carried out.

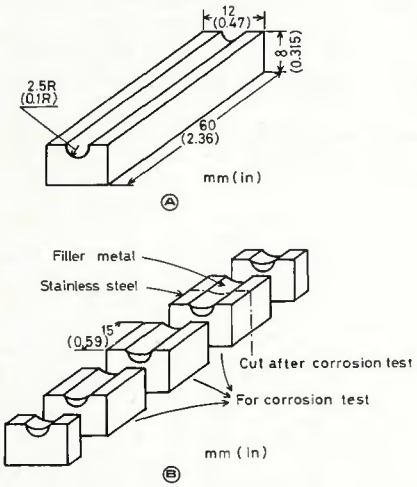

Fig. 1—Shape and size of stainless steel (A), and corrosion test specimen (B)

Experimental Results

Microstructure and Corrosion Morphology

The microstructure of filler metals is shown in Fig. 2. The BAg-6 consisted of α-Cu primary phase and eutectic structure (α_1-Ag + α-Cu). BAg-5 and BAg-4 consisted mainly of α-Cu primary phase and eutectic structure; however, in many instances very small amounts of β phase is observed by x-ray diffraction analysis. The microstructure of CF-12 is markedly different from others due to the existence of β phase. Continuous crystallization of α-Cu primary phase at the braze interface is dominant in BAg-4 brazed specimens.

The morphology of corrosion can be grouped in three types—Fig. 3. All specimens underwent corrosion in the filler metal and interface. The former was the selective dissolution of α-Cu phase in filler

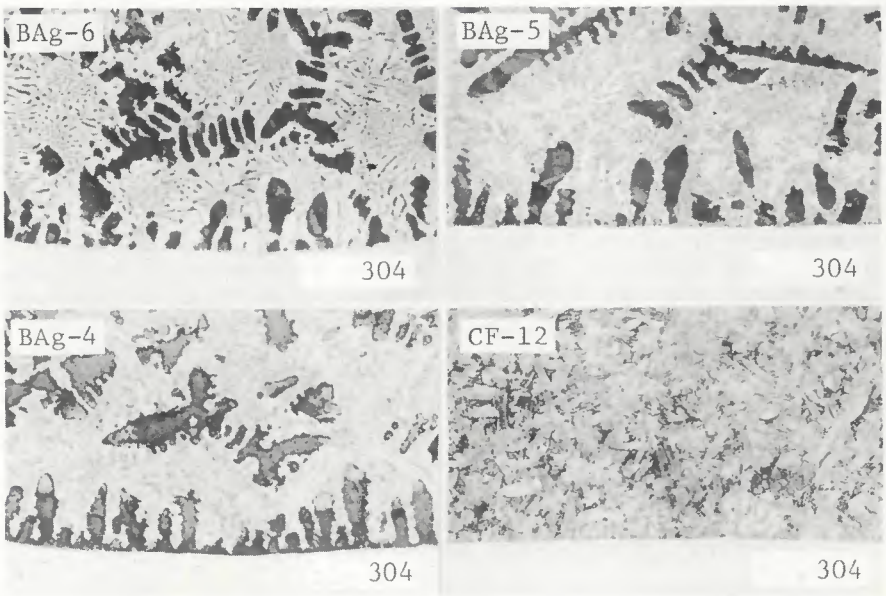

Fig. 2—Microstructure of brazed specimens, Type 304 stainless steel base metal. ×500

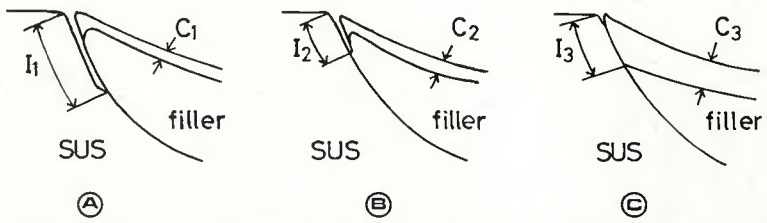

Fig. 3—Schematic illustration of corrosion, interfacial corrosion at stainless steel side (A), both stainless steel and filler metal (B), and dominant corrosion of filler metal (C)

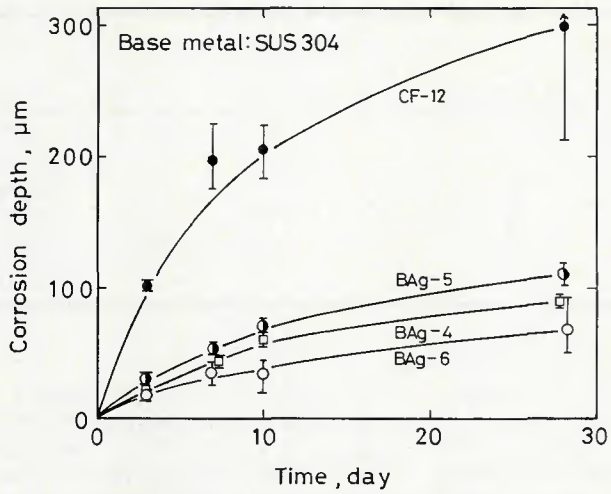

Fig. 4—Corrosion depth of filler metals brazed with Type 304 stainless steel

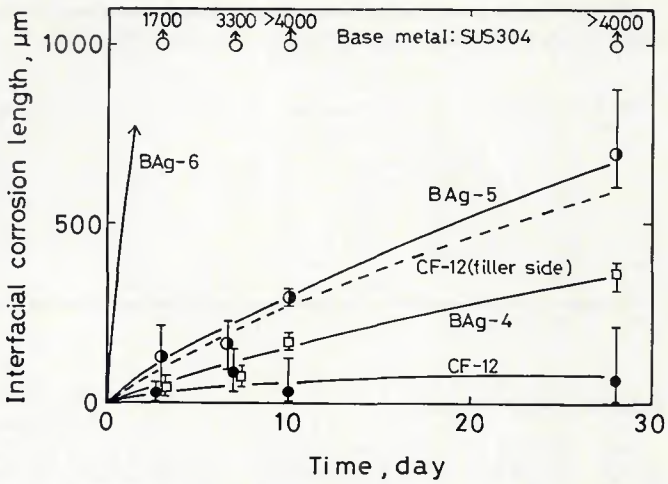

Fig. 5—Effect of filler metal on interfacial corrosion length

metals, similar to the dezincification of α-brass (Refs. 8,9), and proceeded almost homogeneously from its surface.

The corrosion path in the latter was somewhat complicated, depending on the filler metal composition. In BAg-6 and BAg-5 brazed specimens, the path was stainless steel side (Fig. 3A), in BAg-4 the paths were both α-Cu phase crystallized along interface and stainless steel (Fig. 3B), and in CF-12 the corrosion of filler metal from its surface was dominant—Fig. 3C. As a basic principle, the interfacial corrosion length means the length of l_1 and l_2, but in CF-12, l_3 was also measured.

Effect of Filler Metal Composition

The results of corrosion tests on Type 304 stainless steel base metal brazed by different filler metals are shown in Fig. 4. Almost parabolic corrosion depth-immersion time relations are shown. Corrosion resistance decreased in this order: BAg-6, BAg-4, BAg-5, and CF-12.

The copper content in the filler metals may be regarded as having been constant. It is when zinc content was increased that filler metal became less corrosion resistant. In other words, silver-rich filler metal had superior corrosion resistance compared to zinc-rich. Owing to the less corrosion resistant β phase (Refs. 8, 10, 11, 12), CF-12 showed deep corrosion depth. The substitution of 2% Zn in CF-12 for 2% Ni in BAg-4 improved the corrosion resistance remarkably.

In contrast to the corrosion depth experienced with filler metals, the interfacial corrosion length on the stainless steel side increased with increasing filler metal silver content—Fig. 5. Here interfacial corrosion proceeded mainly along base metal. The broken line for CF-12 brazed specimens shows the interfacial corrosion length on the filler metal side (l_3 in Fig. 2). Due to the specimen shape and high corrosion rate for CF-12 filler metal, corrosion from the filler metal surface resulted in a long interfacial corrosion length. From a practical viewpoint, corrosion at the braze interface may have significance and control joint life because it proceeds faster than the corrosion of filler metal. Within the range of the investigation reported here, BAg-4 filler metal will be desirable for practical use.

Effect of Stainless Steel Composition

The effect of base metal composition on the corrosion depths of BAg-4 and 5 is represented in Fig. 6. BAg-4 is more corrosion resistant than BAg-5 on all base metals. The depth of BAg-5 becomes great when combined with Type 310S stainless steel containing much (Ni + Cr). BAg-4 shows a similar tendency, but the dependency on base metal is slight. The fact that the corrosion depth of filler metal depends on the base metal composition suggests the existence of a galvanic cell between the stainless steel surface (which is stable in test solution except at the braze interface) and filler metal—especially the preferentially attacked α-Cu phase.

Interfacial corrosion length decreased in high (Ni + Cr) content base metals such as Types 310S, and 309 stainless steel—Fig. 7. The decrease is larger for BAg-5 filler metal than for BAg-4. Since the stainless steel base metal suffered corrosion at the braze interface, the interfacial corrosion resistance should depend on that of the base metal.

The results shown in Fig. 7 coincided well with the above idea, because the high Ni + Cr content base metal showed good interfacial corrosion resistance. The interfacial corrosion length brazed with BAg-4 has a slight dependence on base

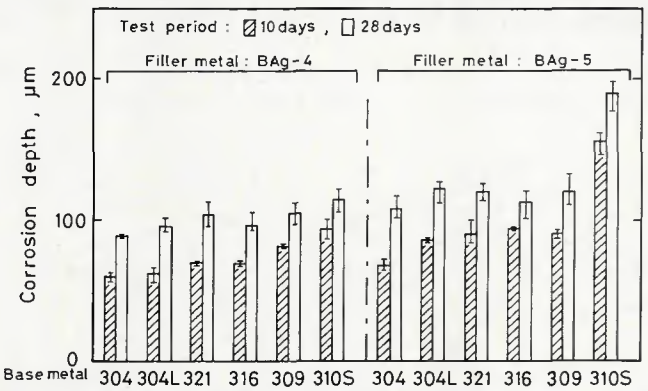

Fig. 6—Effect of base metal on corrosion depth of filler metal

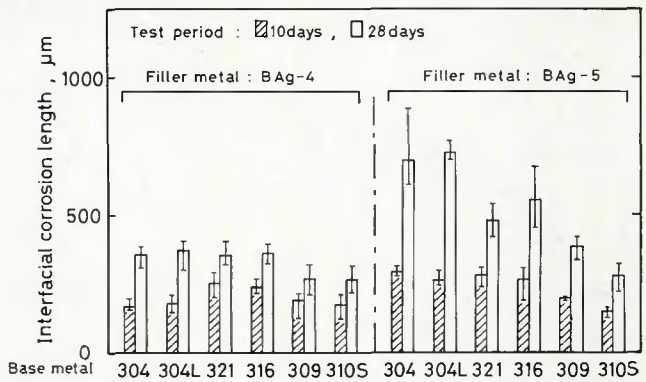

Fig. 7—Effect of base metal on interfacial corrosion length

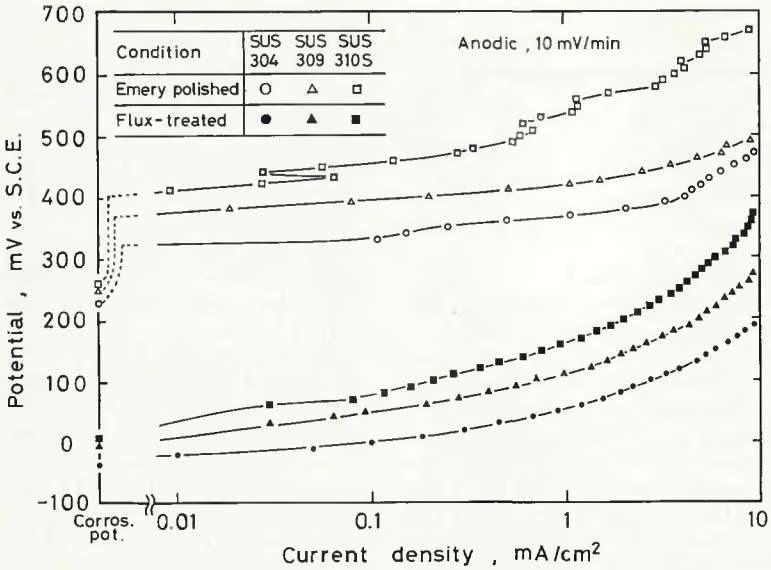

Fig. 8—Effect of flux treatment on anodic polarization curves of stainless steels

metal composition. As a rule, however, base metals with high Ni + Cr contents exhibited superior corrosion resistance. Specimens brazed with BAg-4 filler metal showed superior corrosion resistance to those brazed with BAg-5, and the improvement effected by the nickel addition to filler metal was noticeable when the base metals such as Types 304 and 304L stainless steels with low Ni + Cr contents were used.

Effect of Brazing Flux

Stainless steels are brazed with filler metals after removal of corrosion resistant passive films by the use of aggressive brazing flux. To investigate the effect of flux on the corrosion resistance of stainless steels, anodic polarization curves were measured, using the previously flux-treated stainless steels.

For the flux-treatment investigation, the stainless steel base metal plates were covered with brazing flux and heated at 830°C (1526°F) for 1 min then air cooled and rinsed sufficiently in warm water. Anodic polarization curves are shown in Fig. 8. Here, the corrosion potentials of flux-treated stainless steels representing the braze interface are lower than those with emery polished surfaces. The flux-treated stainless steels show low pitting potentials and large anodic current at low potentials, indicating they are active. The flux-treated surface is repassivated immediately by the oxygen in air when flux residues are removed.

Taking the repassivation of the flux-treated surface into consideration, the stainless steel at the braze interface should be more active than indicated by the curves in Fig. 8. Therefore, it is clear that the use of the brazing flux is one of the causes of interfacial corrosion of brazed stainless steels. Figure 8 also indicates that high Ni + Cr content stainless steels have higher pitting potentials, corresponding well with the interfacial corrosion resistance.

Discussion

Galvanic Effect

The corrosion depth of filler metal was dependent on base metal composition, and the interfacial corrosion length on the base metal side was affected by filler metal composition. These phenomena suggest the operation of galvanic cells between them.

The filler metals consisted of at least two phases—a silver-rich α_1-Ag phase and copper-rich α-Cu phase. Stainless steels are brazed with filler metals after removal of the corrosion resistant passive films by the use of aggressive brazing flux as already indicated in Fig. 8. Thus, the braze interface on the stainless steel side is less corrosion resistant than the bulk stainless steel surface. Therefore, the galvanic effect among the following four phases are expected: stainless steel surface; α_1-Ag phase; flux-affected active stainless steel at braze interface; and α-Cu phase.

Experimental results indicating that the corrosion depth of filler metal was influenced by base metal suggest the formation of a galvanic cell between stainless steel surface (cathode) and α-Cu phase (anode). Also the interfacial corrosion dependence on filler metal composition may arise from the cell between α_1-Ag phase (cathode) and stainless steel at braze interface (anode).

To investigate the galvanic effect, the composition of α_1-Ag and α-Cu phases in each filler metal should be estimated. For this purpose, the lattice parameters of Ag-Cu-Zn ternary alloys (BAg-6 and 5, and CF-12) were measured using an x-ray diffractometer (CuKα, Ni filter, 35kV, 15mA); this was done because the eutectic structure is too fine to measure the composition exactly by electron probe microanalyzer. Furthermore, the diffraction lines of each phase were relatively broad, indicating composition fluctuation. To estimate the average composition, analysis by X-ray diffraction was adopted.

The lattice constant of each phase is derived from the plots of lattice parameter and $\sin^2 \Theta$ (Θ defined as Brag angle). Assuming that the change of lattice constant obeys the principle of additivity, the lattice constant (Å) of each phase is represented by the following equations (Ref. 13).

$$a_{\alpha\text{-Cu}} = 3.6151 + 0.00585\,[\text{at-\% Zn}] + 0.00243\,[\text{at-\% Ag}] \quad (1)$$

$$a_{\alpha_1\text{Ag}} = 4.0857 - 0.00365\,[\text{at-\% Zn}] - 0.00186\,[\text{at-\% Cu}] \quad (2)$$

According to the Ag-Cu-Zn ternary phase diagram (Ref. 14), the concentration of silver and copper distributed in α-Cu and α_1-Ag phase may be regarded as 3 wt-% for each phase; the zinc content is calculated from equations (1) and (2) and the obtained lattice constant.

The results are shown in Table 3. Here

Table 3—Estimated Composition of α-Cu and α_1-Ag Phase in Each Filler Metal, Wt-%

	α_1-Ag phase				α-Cu phase			
Filler metal	Lattice constant, Å	Ag	Zn	Cu	Lattice constant, Å	Cu	Zn	Ag
BAg-6	4.0445	89	8	3	3.7220	66	31	3
BAg-5	4.0143	77	20	3	3.7225	57	40	3
CF-12	4.0065	74	23	3	3.7000	57	40	3

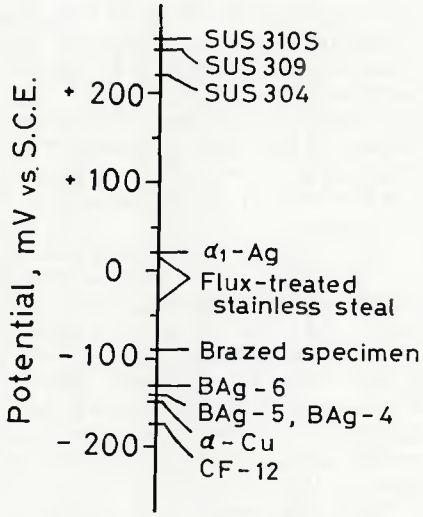

Fig. 9—Corrosion potentials of various phases

the 40% Zn in α-Cu phase of BAg-5 and CF-12 is almost the solubility limit (Refs. 14, 15). Therefore, it was to be expected that zinc additions to CF-12 would allow the existence of much β phase. Zinc in α_1-Ag phase increased in the following order: BAg-6, BAg-5, CF-12. This coincided with the order of zinc content in filler metals.

Potential Measurements

The corrosion potentials of the alloys and brazed specimens were measured—Fig. 9. Saturated calomel electrode (S.C.E.) was used as a reference electrode. The potentials of stainless steel base metal and α_1-Ag phase are shown to be higher than potentials for filler metals and α-Cu phase. The corrosion potential of the brazed specimen was about −80~ −100mV (S.C.E.) irrespective of base metal and filler metal compositions.

Potential measurements revealed that stainless steel and α_1-Ag phase have the ability to act as effective cathodes. The potentials of previously flux-treated stainless steels were higher than brazed specimens, indicating that the phases are relatively stable in the test solution. But as already mentioned, the flux treated surface was repassivated. Considering the repassivation of the flux treated specimen, the potential at the braze interfaces should be much lower and more active than observed ones.

Current between α_1-Ag Phase and Stainless Steel

Galvanic currents between α_1-Ag phases (Ag-Zn-3Cu alloys) of various zinc contents and stainless steels were measured by obtaining the polarization curves between them. The contact current between the α_1-Ag phase cathode and flux-treated stainless steel anode depends on the zinc content in α_1-Ag phase—Fig. 10. The positive current in Fig. 10 means that α_1-Ag phases are cathodes and that the flux-treated stainless steels are anodes.

The increase in zinc content decreased the galvanic current between the α_1-Ag phase and flux-treated stainless steel. Therefore, the low zinc content α_1-Ag phase in BAg-6 (Table 3) seems to be responsible for the increased interfacial corrosion; however, the contact current dependence of zinc is somewhat slight in the range of 8 ~ 23% Zn. In addition, due to the high silver content of BAg-6, the surface area of the α_1-Ag phase is larger than that of BAg-5 and CF-12. An increase of cathode area provides large anodic current density. Thus, the reason for the marked increase in the interfacial corrosion length in stainless steel brazed with high silver content BAg-6 filler metal may be attributed to the increase of contact current due to the decrease of zinc in α_1-Ag phase and the increase of cathode area (amount of α_1-Ag phase) by the increase of silver content.

Current between Stainless Steels and α-Cu Phase

The galvanic current between the stainless steel (emery polished) and α-Cu phase (Cu-31Zn-3Ag alloy) was measured to clarify the effect of stainless steel composition on the corrosion of filler metal. Furthermore, the galvanic current between the emery polished and flux-treated stainless steels was also measured. The results are shown in Table 4.

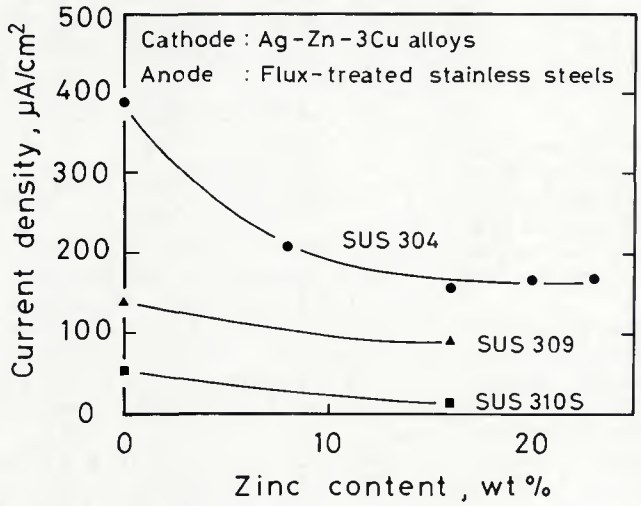

Fig. 10—Contact current between α_1-Ag phases with different zinc content and flux-treated stainless steels

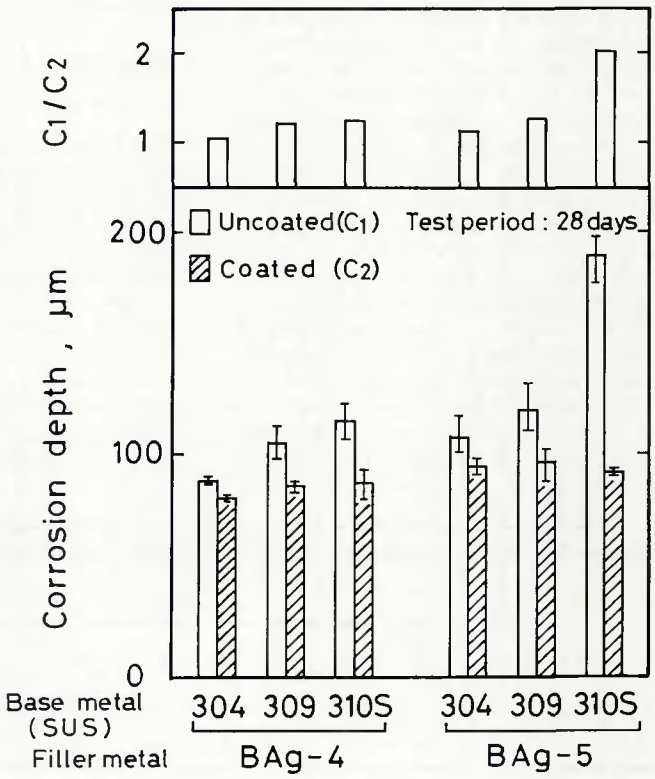

Fig. 11 (right)—Effect of stainless steel surface on corrosion depth of filler metals

Table 4—Galvanic Current Measured By Polarization Curves, Surface Area Ratio Of Cathode to Anode Is Unity

Type stainless steel cathode[a]	Anode	Current density $\mu A/cm^2$	($\mu A/in.^2$)
304 (Emery polished)	Cu-31Zn-3Ag[a]	110	(710)
309 (Emery polished)	Cu-31Zn-3Ag[a]	130	(840)
310S (Emery polished)	Cu-31Zn-3Ag[a]	150	(970)
304 (Emery Polished)	Type 304[b]	100	(650)
309 (Emery Polished)	Type 309[b]	85	(550)
310S (Emery Polished)	Type 310S[b]	85	(550)

(a) Emery polished.
(b) Flux treated.

Here it may be seen that the stainless steel surface acts as an effective cathode to the α-Cu phase, indicating that the stainless steel surface accelerates the corrosion of filler metal.

The cathodic effect of the stainless steel surface is also clear from the results of experiments indicating that the corrosion depth of filler metal was unaffected when the stainless steel surface was covered by silicon resin—Fig. 11. The corrosion depths of filler metal with coated base metal were almost the same, irrespective of the base metal composition. The corrosion resistance of BAg-4 is always superior to that of BAg-5. The C_1/C_2 ratio of the corrosion depth of filler metal with uncoated base metal (C_1) to coated base metal (C_2) increased with the increase in Ni + Cr content of base metal; this indicated that the corrosion depth increased through contact with high Ni + Cr content stainless steel, coinciding well with the galvanic current measurement.

The above results confirm that the presence of stainless steel—especially high Ni + Cr content stainless steels—accelerates the corrosion of filler metal. Galvanic current between emery polished and flux-treated stainless steels is not changed with Ni + Cr content. This means that the high Ni + Cr content stainless steel is less susceptible to the flux treatment due to its high corrosion resistance, even though its surface has a great affinity for cathodic effects.

Figure 12 shows the cathodic effects of a stainless steel surface and α_1-Ag phase. Increasing the Ni + Cr content in the stainless steel or the silver content in the filler metal shifts the cathodic polarization curve from A to B as indicated by an arrow. The shift increases the anodic current from i_A to i_B and gives large corrosion depth of filler metals and interfacial corrosion length.

Improvement by Quenching

The results of experimentation suggest that homogeneous distribution of filler metal composition relieves the galvanic current between filler metal and stainless steel. Quenching from high temperature after the flow of filler metal yields saturated α-Cu and α_1-Ag phase. This means that α-Cu phase with high silver and α_1-Ag phase with high copper are coexistent. This may relieve the galvanic current between α_1-Ag phase and stainless steel at the interface, and between stainless steel surface and α-Cu phase.

The results of corrosion tests on quenched specimens brazed with BAg-4 and 5 filler metals are shown in Figs. 13 and 14. The corrosion of both the filler metal and the interface are improved by quenching. However, the application of quenching for commercial use seems to be somewhat impractical because quenching may yield torsion and because of the difficulty of quenching temperature control. On the other hand, it is noteworthy that quenching is effective in improving the corrosion resistance of stainless steels brazed with silver-base filler metals.

Effect of Nickel Addition

Nickel has been known as a dezincification suppressing element for brass (Ref. 10). Fortunately, nickel added to a ternary alloy is preferentially distributed in the α-Cu phase (Fig. 15), because both silver and zinc have little solubility of nickel (Ref. 16). The nickel content in the α-Cu phase of BAg-4 is estimated to be 4.7% when neglecting the mutual solubility between α_1-Ag and α-Cu phase and zinc fluctuation. Nickel in α-Cu phase appears to be effective for the suppression of dezincification type corrosion. A similar effect was confirmed in Ag-Cu-Cd-Zn-Ni BAg-3 type filler metal (Ref. 4).

Nickel in filler metal affects interfacial corrosion. Figure 16 shows the line analysis of nickel, chromium and iron at a brazed interface. The nickel-depleted zone was formed by the use of nickel-less filler metals, irrespective of stainless steel composition; however, the addition of 2%Ni (BAg-4) prevented the formation of a nickel-depleted zone over a depth of several microns.

The line profiles of chromium and iron are homogeneous and decreased drastically only at the interface. However, the nickel-depleted zone changed into ferrite phase—Table 5. The composition of the nickel-depleted zone in Type 304 stainless steel is similar to that of Type 430 stainless steel. The corrosion potential of flux treated Type 430 stainless steel was less than −660 mV (S.C.E.) and showed large anodic current under small anodic polarization by a potentiostat. This served to confirm that the phase is less

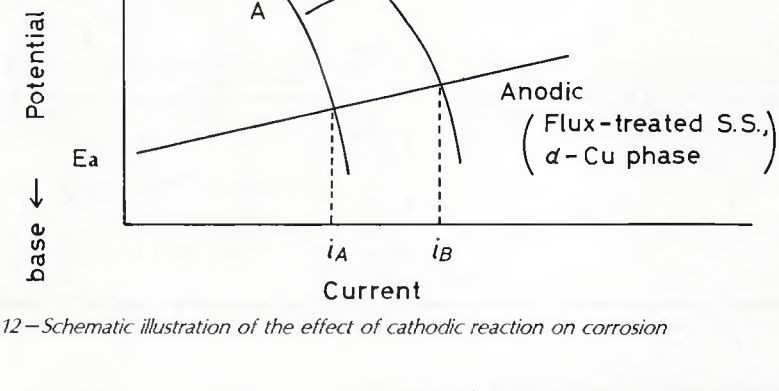

Fig. 12—Schematic illustration of the effect of cathodic reaction on corrosion

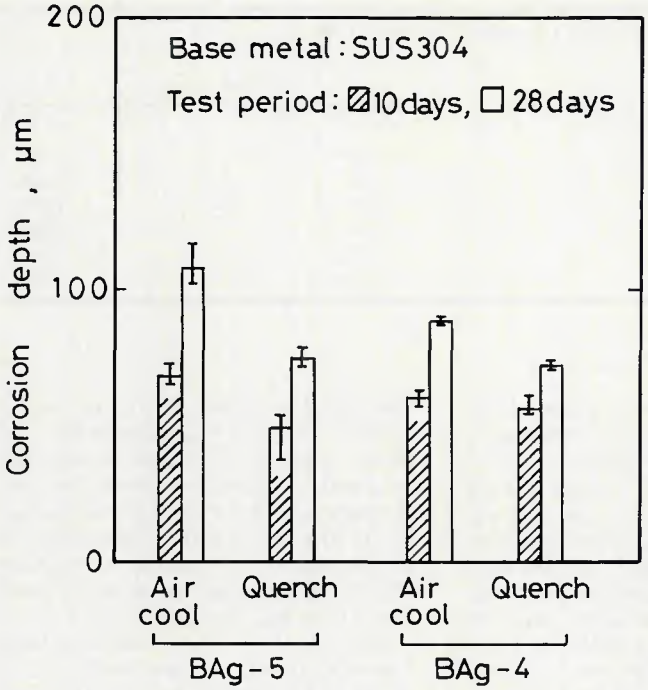

Fig. 13—Improvement of corrosion depth of filler metals by quenching

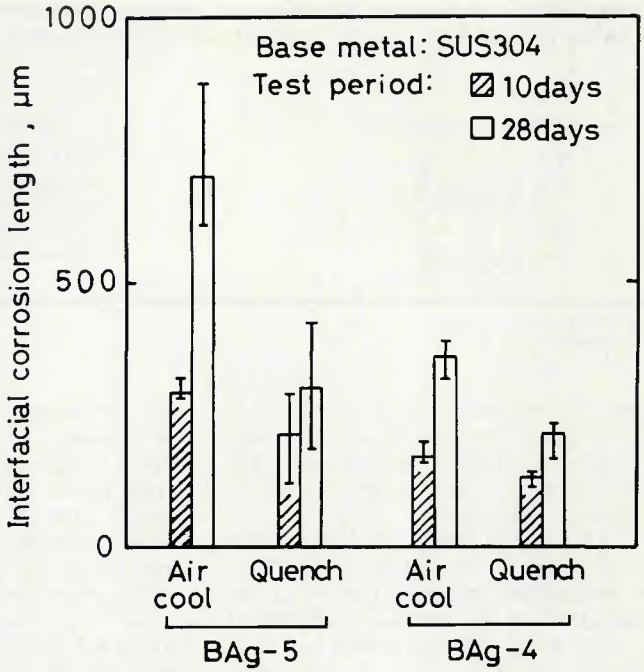

Fig. 14—Improvement of interfacial corrosion length by quenching

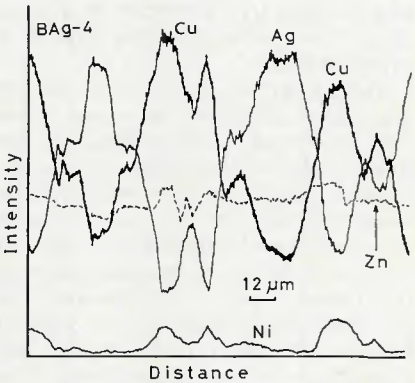

Fig. 15—Line analysis of BAg-4 by electron probe micro-analyzer

corrosion-resistant than nickel containing ones.

Instead of nickel, filler metal constituents (Ag,Zn,Cu) are observed in the zone. The formation rate of the nickel-depleted zone is controlled by the diffusion of nickel in austenitic stainless steel (Ref. 17). Nickel depletion may be attributed to the fact that the molten filler metal has extensive solubility only for nickel. Thus, the addition of nickel in filler metal prevented the dissolving of nickel in filler metal and also prevented the formation of a nickel-depleted zone. The effect of nickel in filler metal on the improvement of the interfacial corrosion is attributed to the prevention of formation of a less corrosion resistant nickel-depleted zone at braze interface.

Even in nickel bearing filler metals, however, stainless steel suffers interfacial corrosion. It may be attributable to the use of brazing flux which leaves the active thin layer free of protective passive films. In addition, once interfacial corrosion starts due to the galvanic effect, corrosion may proceed by the aid of the oxygen concentration cell between the penetrating corrosion tip and the surface bulk area.

Conclusion

Investigation on the effect that brazing with silver-base filler metal and stainless steel compositions have on the corrosion behavior of brazed joints in chloride solution led to the following:

1. In ternary Ag-Cu-Zn silver-base filler metals with almost equal copper, an increase of silver (*i.e.,* decrease of zinc) improves the corrosion resistance of the

Table 5—X-Ray Diffraction Analysis of Stainless Steel Base Metals and Nickel-Depleted Zones, (CoKα, Fe filler, 40kV, 20mA)[a]

Observations														Calculations				
														Austenite		Ferrite		
Emery polished, after brazing heat cycle						Nickel-depleted zone												
Type 304		Type 309		Type 310S		Type 304		Type 309		Type 310S		Fe-16.1Cr-12.0Ni	Fe-23.39Cr-21.39Ni	Fe-18.1Cr	ASTM data for pure α-Fe	
d	I	d	I	d	I	d	I	d	I	d	I	d	d	d	d	(hkl)
2.070	VS	2.073	S	2.073	S	2.070	VS	2.073	W	2.073	W	2.069	2.071			
						2.029	S	2.031	S	2.033	S			2.031	2.0268	110
1.794	M	1.798	M	1.798	M	1.794	M	1.798	vw	1.798	vw	1.792	1.794			
						1.438	W	1.438	vw	1.438	vw			1.436	1.4332	200
1.269	M	1.270	W	1.271	W	1.269	W									

(a) d—spacing, Å; I—intensity, VS > S > M > W > vw

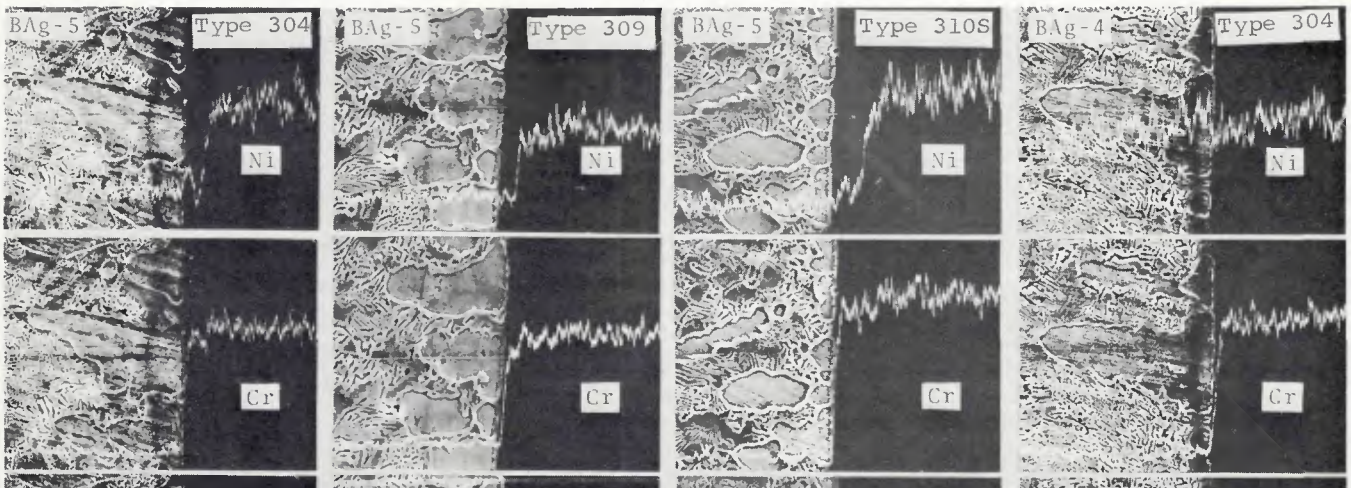

Fig. 16 — Line analysis of nickel, chromium and iron at brazed interface showing nickel-depleted zone in stainless steels brazed with nickel-less filler metals. ×960 (reduced 26% on reproduction)

filler metal, itself; however, it increases the interfacial corrosion on the stainless steel side.

2. The substitution of Type 304 base metal for high Ni + Cr content stainless steels (such as Type 310S) increases the corrosion of filler metal but decreases the interfacial corrosion.

3. Corrosion depth dependency on the base metal and interfacial corrosion length dependency on the filler metal composition are explainable in terms of the galvanic effect between the α-Cu phase and stainless steel surface, and between the flux-affected stainless steel (nickel-depleted zone) at the braze interface and α_1-Ag phase, respectively.

4. A nickel-depleted zone is formed in stainless steel at the braze interface when nickel-free filler metal is used. The zone showed ferrite structure. The zone and the removal of passive films by brazing flux are believed to be responsible for the enhanced interfacial corrosion.

5. The addition of nickel in filler metal relieves the interfacial corrosion by preventing the formation of a less corrosion resistant nickel-depleted zone in the stainless steel at the brazed interface.

6. Quenching the specimen is effective for the improvement of the corrosion resistance of a brazed joint.

Acknowledgment

The authors would like to thank Mr. Chikara Fujiwara for the experimental work.

References

1. Sistare, G.H., Halbig, J.J., and Grenell, L.H. 1954. Silver brazing alloys for corrosion-resistant joints in stainless steels. *Welding Journal* 33 (2):137-143.

2. Kawakatsu, I. 1973. Corrosion of BAg brazed joints in stainless steel. *Welding Journal* 52 (6):233-s to 239-s.

3. Stock, D. C., and Smellie, W. J. 1960. Soldering stainless steels. *Welding and Metal Fabrication* 23(4):160-161.

4. Mahler, W., und Zimmerman, K. F. 1977. Beitrag zur Frage der Meerwasserbestandigkeit von Hartlotverbindungen-Entzinkungskorrosion. *Metall* 31(9):971-974.

5. Jarman, R. A., Myles, J. W., and Booker, C. J. L. 1973. Interfacial corrosion of brazed stainless steel joints in domestic tap water. *British Corrosion Journal* 8(1):33-37.

6. Herbsleb, G. und Schwenk, W. 1975. Korrosionsverhalten von Edelstahlrohren und Rohrverbindungen bei der Warmwasserverteilung in der Hausinstallation. *Werkstoffe und Korrosion* 26(2):93-103.

7. Steffens, H. D., Richer, B., und Lange, H. 1975. Einfluss korrosiver Medien auf die Lebensdauer hartgeloter Verbindungen (Teil I). *Werkstoffe und Korrosion* 26(11):836-843.

8. Langenegger, E. E., and Robinson, F. P. A. 1969. A study of the mechanism of dezincification of brasses. *Corrosion* 25(2):59-66.

9. Natarajan, R., Angelo, P. C., George, N. T., and Tamhankar, R. V. 1975. Dezincification of cartridge brass. *Corrosion* 31(8): 302-303.

10. Roges, T. H., 1968. *Marine Corrosion:* 118 London: George Newhes Ltd.

11. Butts, A. 1954. *Copper — the science and technology of the Metal, its alloys and compounds.* p. 383. New York: Reinhold Publishing Corp.

12. Poling, G. W., and Notoya, T. 1979. Corrosion pretreatments for copper-zinc alloys. *Corrosion* 35 (1): 33-38.

13. Pearson, W. B. 1967. *A handbook of lattice spacings and structures of materials and alloys:* Oxford: Pergamon Press.

14. Weigert, K. M. 1954. Constitution and properties of Ag-Cu-Zn binary alloys. *Journal of Metals* 6 (2):233-237.

15. Gebhardt, E., Petzow, G., and Krauss, W. 1962. Uber den Aufbau des Systems Kupfer-Silver-Zink. *Z. Metallkde.* 53(6):372-379.

16. Hausen, M. 1958. *Constitution of binary alloys,* New York: McGraw-Hill Book Company.

17. Takemoto, T. and Okamoto, L. 1984. *Quarterly Journal of Japan Welding Society.* 2(2):300-308.